Plutonium Migration during Leaching of Cemented Radioactive Waste Sludges

Supplementary Material

Table S1. Composition of Ordinary Portland Cement and Blast furnace Slag determined by XRF.

Composition	OPC wt. %	BFS wt. %
CaO	67.00	42.83
SiO_2	18.31	34.23
Al_2O_3	4.50	11.67
Fe_2O_3	3.06	1.42
MgO	2.20	0.27
SO_3	3.25	1.73
K_2O	0.74	0.32
Na_2O	0.24	0.16
TiO_2	0.31	0.51

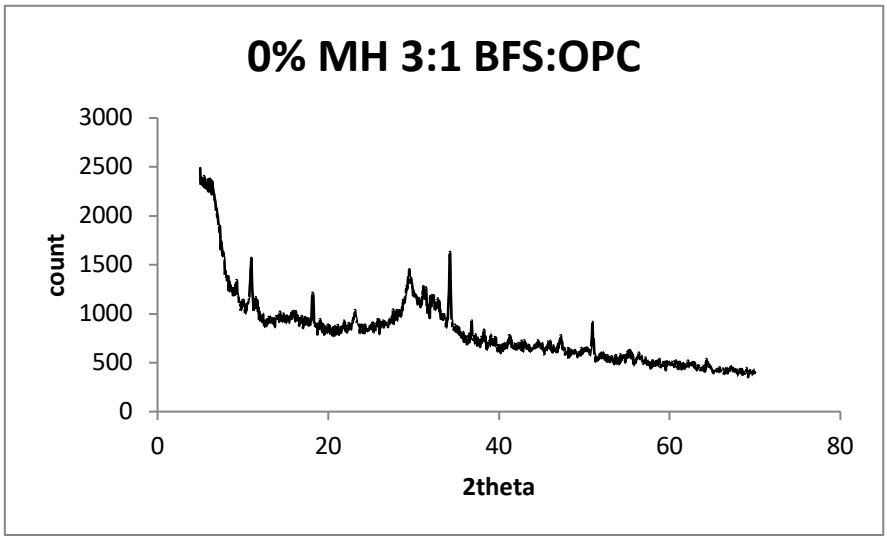

a

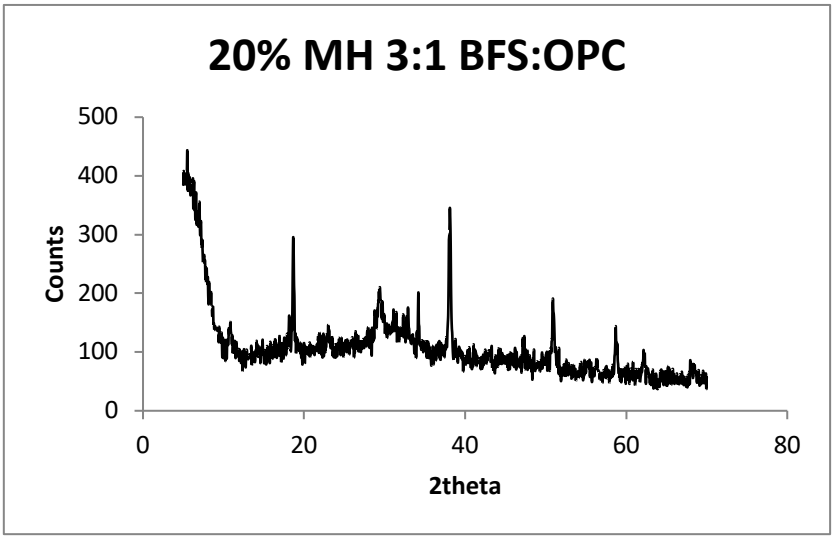

b

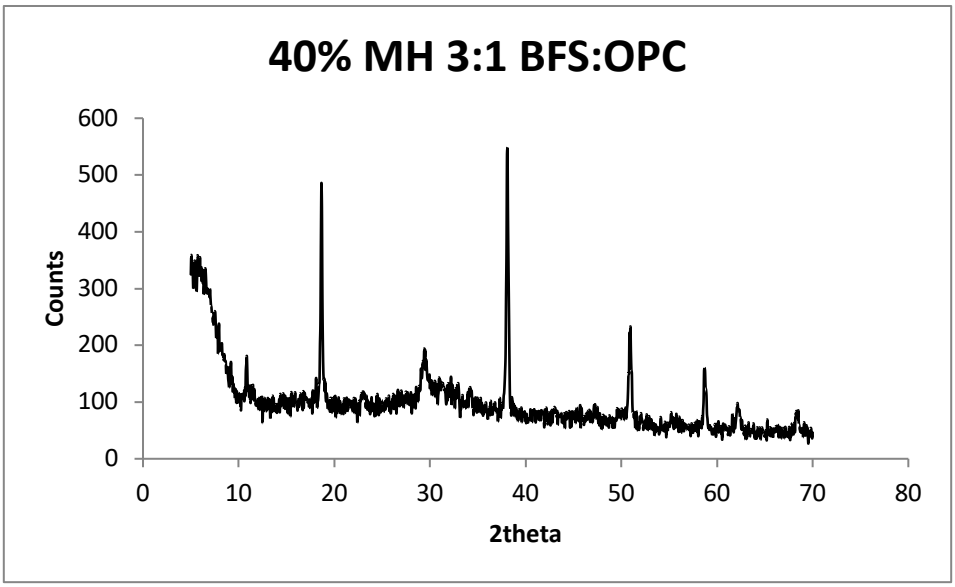
40% MH 3:1 BFS:OPC
Counts
600
500
400
300
200
100
0
0
10
20
30
40
50
60
70
80
2theta

c

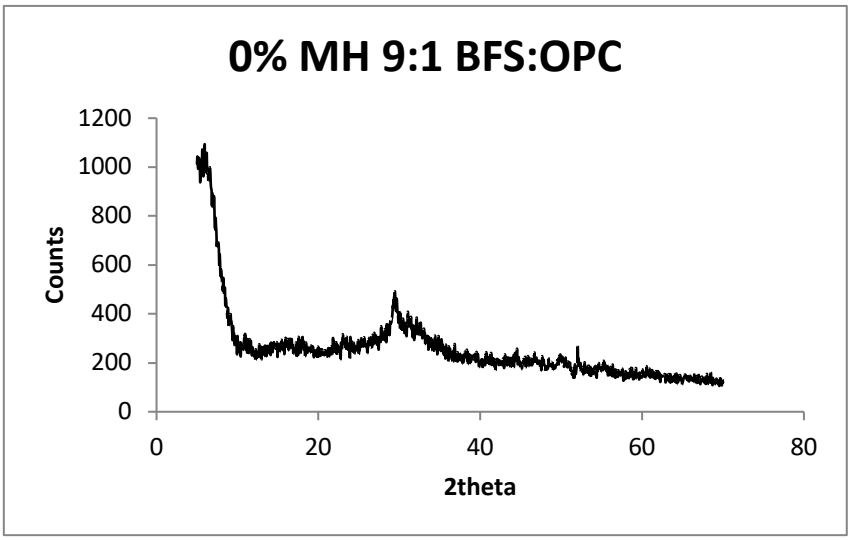
0% MH 9:1 BFS:OPC
Counts
1200
1000
800
600
400
200
0
0
20
40
60
80
2theta

d

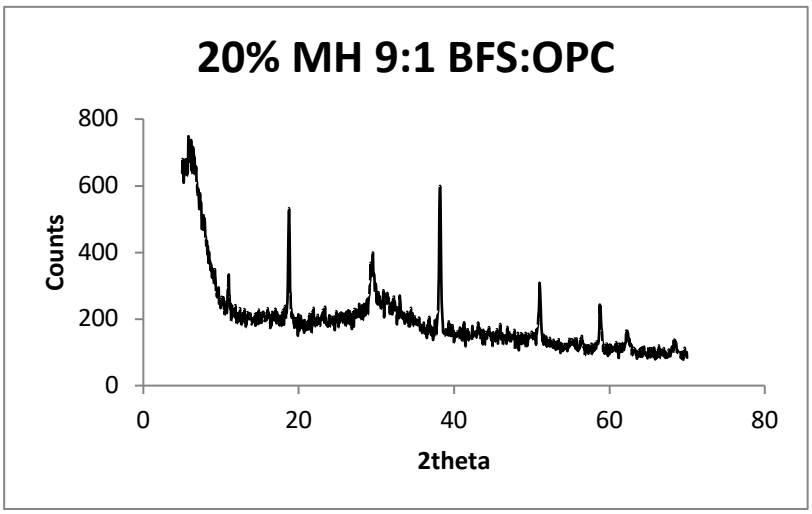
20% MH 9:1 BFS:OPC
Counts
800
600
400
200
0
0
20
40
60
80
2theta

e

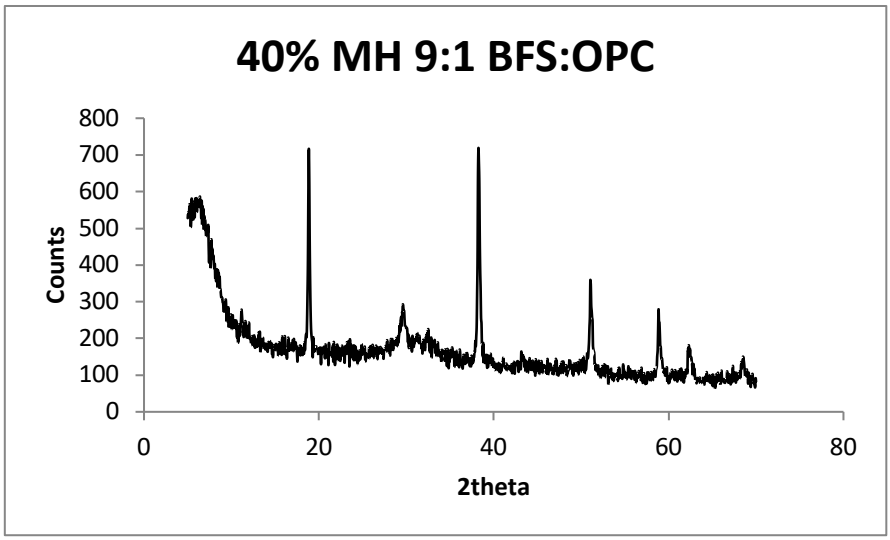
40% MH 9:1 BFS:OPC
Counts
800
700
600
500
400
300
200
100
0
0
20
40
60
80
2theta

f

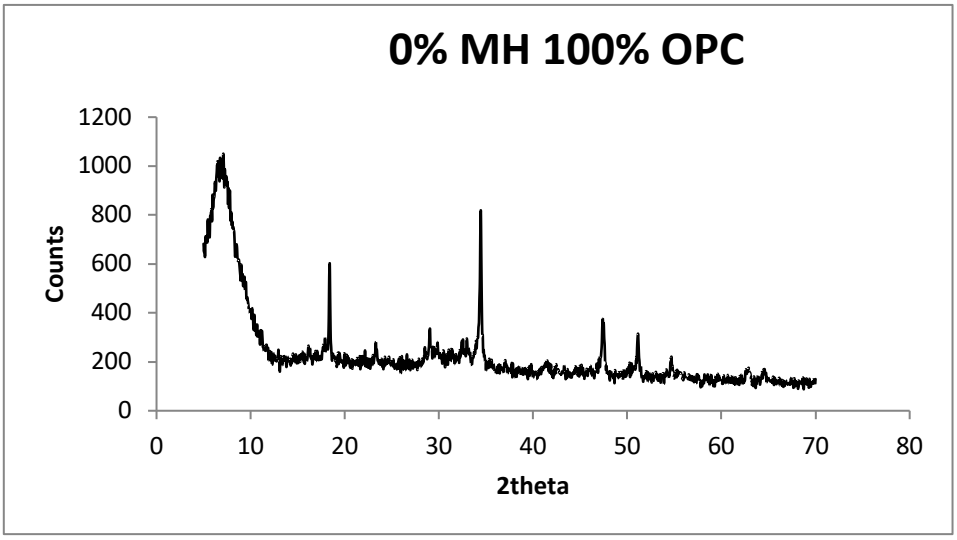
0% MH 100% OPC
Counts
1200
1000
800
600
400
200
0
0
10
20
30
40
50
60
70
80
2theta

g

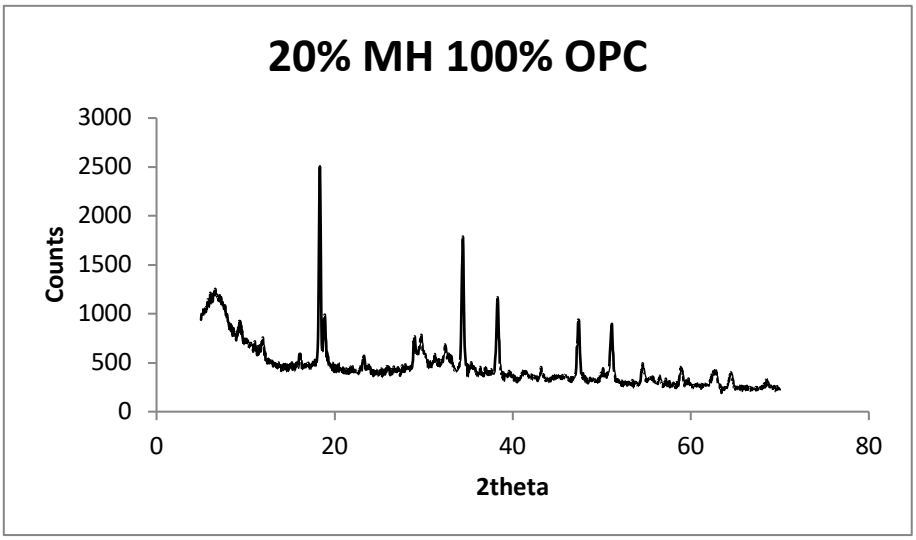
20% MH 100% OPC
Counts
3000
2500
2000
1500
1000
500
0
0
20
40
60
80
2theta

h

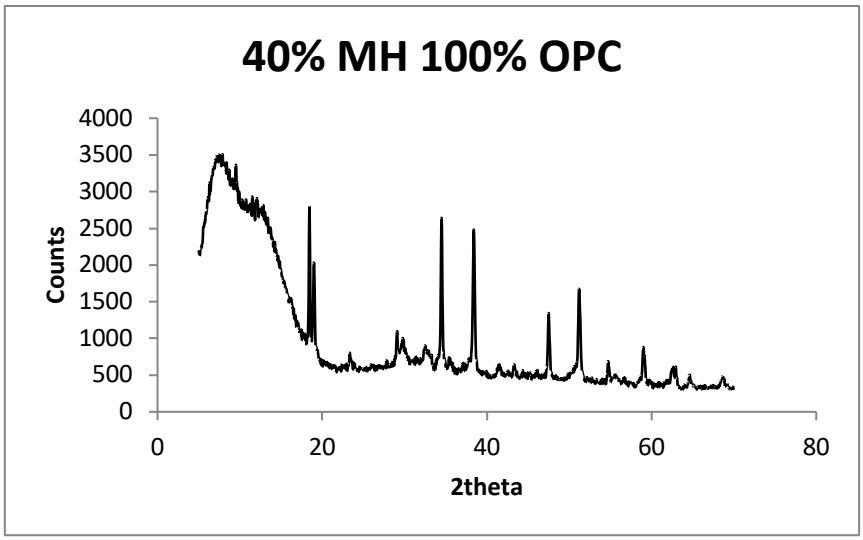

i

Figure S1. Supplementary XRD patterns.

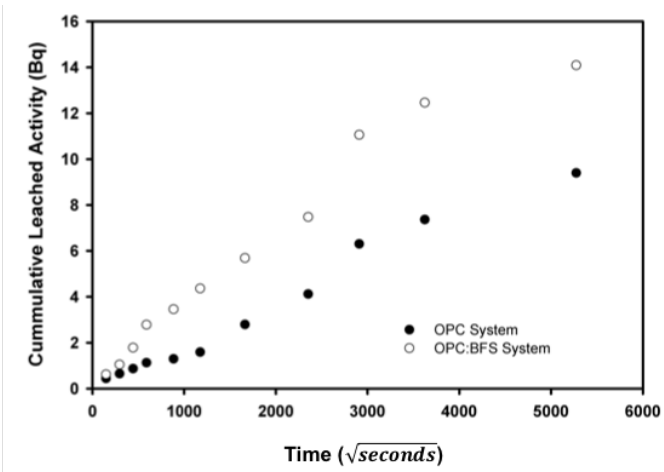

Figure S2. Release of ^{239}Pu from cement samples over time. Samples are 100% OPC and 3:1 BFS:OPC, plotted as cumulative leached activity vs. square root time.

Table S2. Results of linear combination fitting (LCF) using Athena for each of the spectra collected in this study. Summed micro focus spectra for Figure 7 are shown in bold.

		Pu_V		Pu_IV	
Spectrum	**r-factor**	**Weight**	**error**	**Weight**	**error**
S2_1D_Xanes_Side.0004	0.005	**0.638**	0.018	**0.362**	0.018
S2_1D_XANES_scan region.0001	0.009	**0.444**	0.023	**0.556**	0.023
S2_1D_XANES_scan region.0002	0.007	**0.404**	0.022	**0.596**	0.022
S2_1D_XANES_scan region.0003	0.015	**0.410**	0.031	**0.590**	0.031
S2_1D_XANES_scan region.0001	0.039	**0.298**	0.048	**0.702**	0.048
S2_1D_XANES_scan region.0002	0.026	**0.299**	0.040	**0.701**	0.040
S2_1D_XANES_Side.0001	0.014	**0.395**	0.029	**0.605**	0.029
S2_1D_EXAFS_Side.0001	**0.018**	**0.252**	**0.031**	**0.565**	**0.031**
S2_1D_EXAFS_Side.0002	**0.017**	**0.212**	**0.031**	**0.589**	**0.031**
S2_1D_EXAFS_Side.0003	**0.018**	**0.172**	**0.032**	**0.570**	**0.032**
S1_1D_XANES_Centre.0002	0.006	**0.511**	0.020	**0.489**	0.020
S1_1D_EXAFS_Centre.0001	**0.009**	**0.644**	**0.022**	**0.356**	**0.022**
S1_1D_EXAFS_Centre.0002	**0.012**	**0.641**	**0.026**	**0.359**	**0.026**
S1_1D_EXAFS_Centre.0003	**0.011**	**0.629**	**0.025**	**0.371**	**0.025**
S1_1D_EXAFS_Centre.0004	**0.009**	**0.636**	**0.023**	**0.364**	**0.023**
S1_1D_XANES_Centre.0001	0.008	**0.460**	0.023	**0.540**	0.023
S1_1D_XANES_TOP.0001	0.011	**0.553**	0.026	**0.447**	0.026
S4_1D_EXAFS_bottom.0001	**0.013**	**0.766**	**0.026**	**0.234**	**0.026**
S4_1D_EXAFS_bottom.0002	**0.010**	**0.731**	**0.023**	**0.269**	**0.023**
S4_1D_EXAFS_bottom.0003	**0.008**	**0.738**	**0.022**	**0.262**	**0.022**
S4_1D_XANES_Centre.0001	0.026	**0.617**	0.038	**0.383**	0.038
S4_1D_XANES_Side.0001	0.017	**0.542**	0.032	**0.458**	0.032
S4_1D_XANES_Side.0003	0.007	**0.413**	0.023	**0.587**	0.023
S4_1D_XANES_TOP.0001	0.010	**0.439**	0.025	**0.561**	0.025
S4_1D_XANES_bottom.0001	0.008	**0.664**	0.022	**0.336**	0.022
S3_1D_EXAFS_bottom.0001	**0.012**	**0.503**	**0.026**	**0.497**	**0.026**
S3_1D_EXAFS_bottom.0002	**0.015**	**0.537**	**0.029**	**0.463**	**0.029**
S3_1D_EXAFS_bottom.0003	**0.012**	**0.461**	**0.027**	**0.539**	**0.027**
S3_1D_EXAFS_bottom.0004	**0.011**	**0.569**	**0.025**	**0.431**	**0.025**
S3_1D_XANES_Centre.0001	0.036	**0.550**	0.044	**0.450**	0.044
S3_1D_XANES_bottom.0002	0.015	**0.513**	0.030	**0.487**	0.030
S3_1D_XANES_bottom.0003	0.022	**0.608**	0.035	**0.392**	0.035
S3_1D_XANES_side.0001	0.009	**0.488**	0.024	**0.512**	0.024
S3_1D_XANES_top.0001	0.016	**0.486**	0.031	**0.514**	0.031
S3_1D_XANES_top.0002	0.012	**0.476**	0.027	**0.524**	0.027
Mean Short Cure		**0.447**	**0.028**	**0.515**	**0.028**
Mean Long Cure		**0.561**	**0.028**	**0.439**	**0.028**
Mean S1		**0.582**	**0.024**	**0.418**	**0.024**
Mean S2		**0.352**	**0.032**	**0.575**	**0.032**
Mean S3		**0.519**	**0.030**	**0.481**	**0.030**
Mean S4		**0.614**	**0.024**	**0.255**	**0.024**

Table S3. Additional EXAFS fitting parameters and statistics for select samples. Here, $S0^2$ denotes the amplitude reduction factor, N denotes coordination number (shell occupancy), R denotes interatomic distance, σ^2 denotes the Debye-Waller factor and the 'r-factor' denotes the least squared residual for the overall fit. Parameters marked '*' were fixed during the fitting process. Numbers in brackets are the number of spectra summed to provide the dataset for fitting. 'ax' and 'eq' denote axial and equatorial oxygen shells, respectively. Sampling locations are shown in the Supplementary Information Maps 1–18.

Sample	Path	$S0^2$	±	N	R	±	σ^2	±	r-Factor
S2 (3)	$Pu—O_{ax}$	1.11	0.47	0.5*	1.88	0.14	0.01	0.025	0.027
	$Pu—O_{eq}$			6.0*	2.24	0.03	0.01	0.006	
S2 (3)	$Pu—O_{eq}$	0.96	0.11	6.0*	2.25	0.01	0.009	0.002	0.025
	Pu—Pu			3.0*	3.65	0.03	0.011	0.004	
S2 (3)	$Pu—O_{ax}$	1.15	0.24	0.5	1.84	0.07	0.012	0.011	0.021
	$Pu—O_{eq}$			6.00*	2.25	0.2	0.011	0.003	
	Pu—Pu			3.00*	3.65	0.04	0.013	0.005	
S3 (4)	$Pu—O_{ax}$	0.9*		0.5	1.77	0.02	0.003	0.004	0.009
	$Pu—O_{eq}$			6	2.30	0.01	0.007	0.001	
	Pu—Pu			3	3.77	0.03	0.01	0.010	

Supplementary XRF maps

The XRF maps for samples 1–4 are shown in XRF maps 1–18 a schematic of the samples and map locations is also provided below.

The XRF maps are plotted in a scale of raw count rates. Counts have not been corrected for changes in incident flux or absorption by air or sample cell or detector windows. Counts have not been corrected for matrix absorption effects in the samples. The maps have not been used to determine absolute concentrations and are only used to indicate the relative position of Pu and different cement forming phases within each sample.

The relative scale (and plotted colors) for each element within each XRF map have been selected to clearly show the relative concentration of that element within the map. As such the colors between different elements in each map are not comparable and do not indicate relative element concentrations.

Some XRF maps near the edge of samples were affected by sample geometry effects. Rather than observe no fluorescence from positions off the flat, polished surface of the same, fluorescence was observed from the incident beam impinging on the adjacent face of the sample.

For XRF maps of the leached zone appear as a low fluorescence yield stripe in the data, due to the lower elemental concentrations in the samples in this leached zone.

The positions where the Pu XAS spectra were collected are labelled in XRF maps 1–8.

XRF and XAS sampling location data

Schematic of XRF mapping positions on sample 1-4. The dashed line represents the extent of the visibly leached zone of the samples 2 and 3.

Note that the XRF map locations are not to scale due to the small or very narrow map dimension compared to the sample size.

Points selected for XANES and EXAFS analysis are shown by cross hairs on the Plutonium maps.

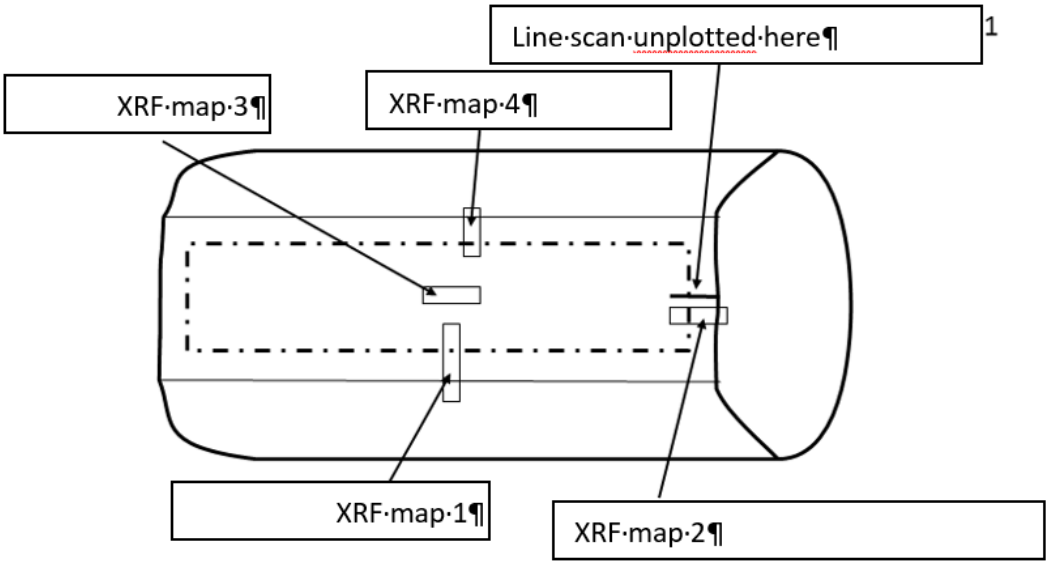

Sample 2—leached sample, short cure.

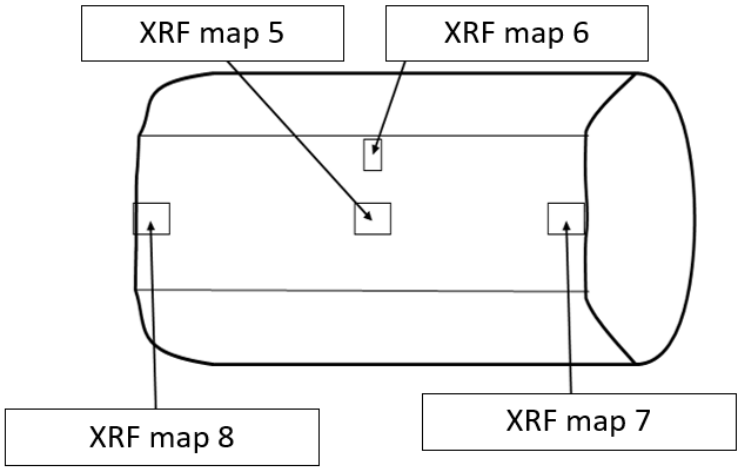

Sample 4—unleached, long cure.

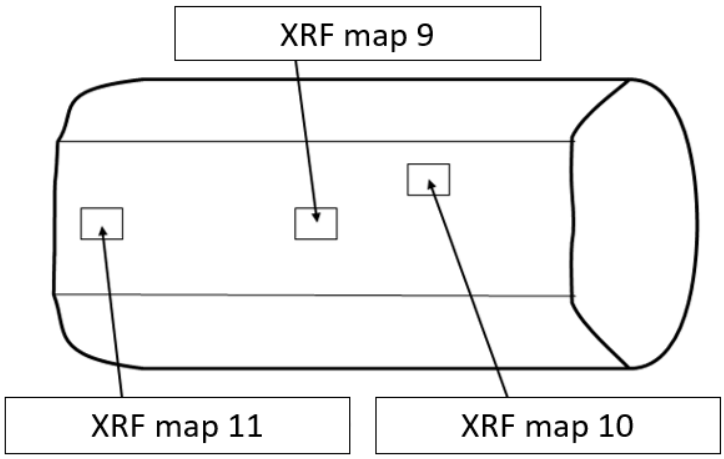

Sample 1—unleached, short cure.

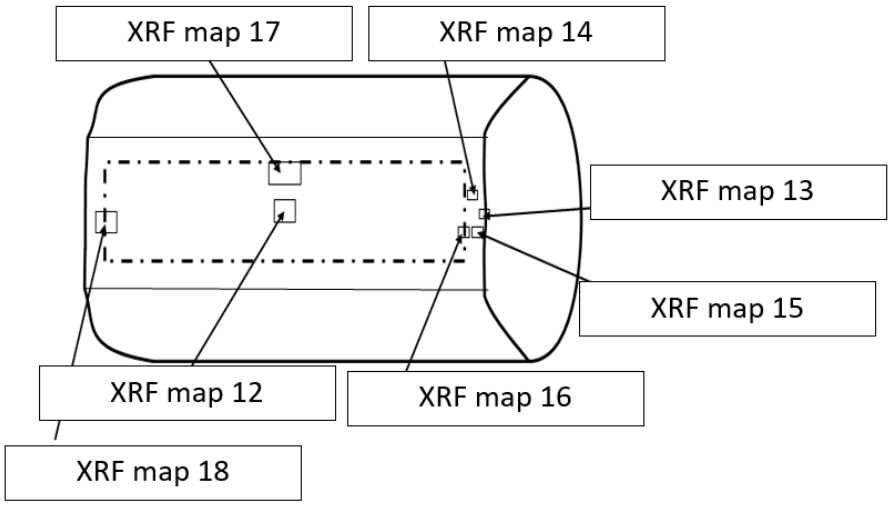

Sample 3—leached, long cure.

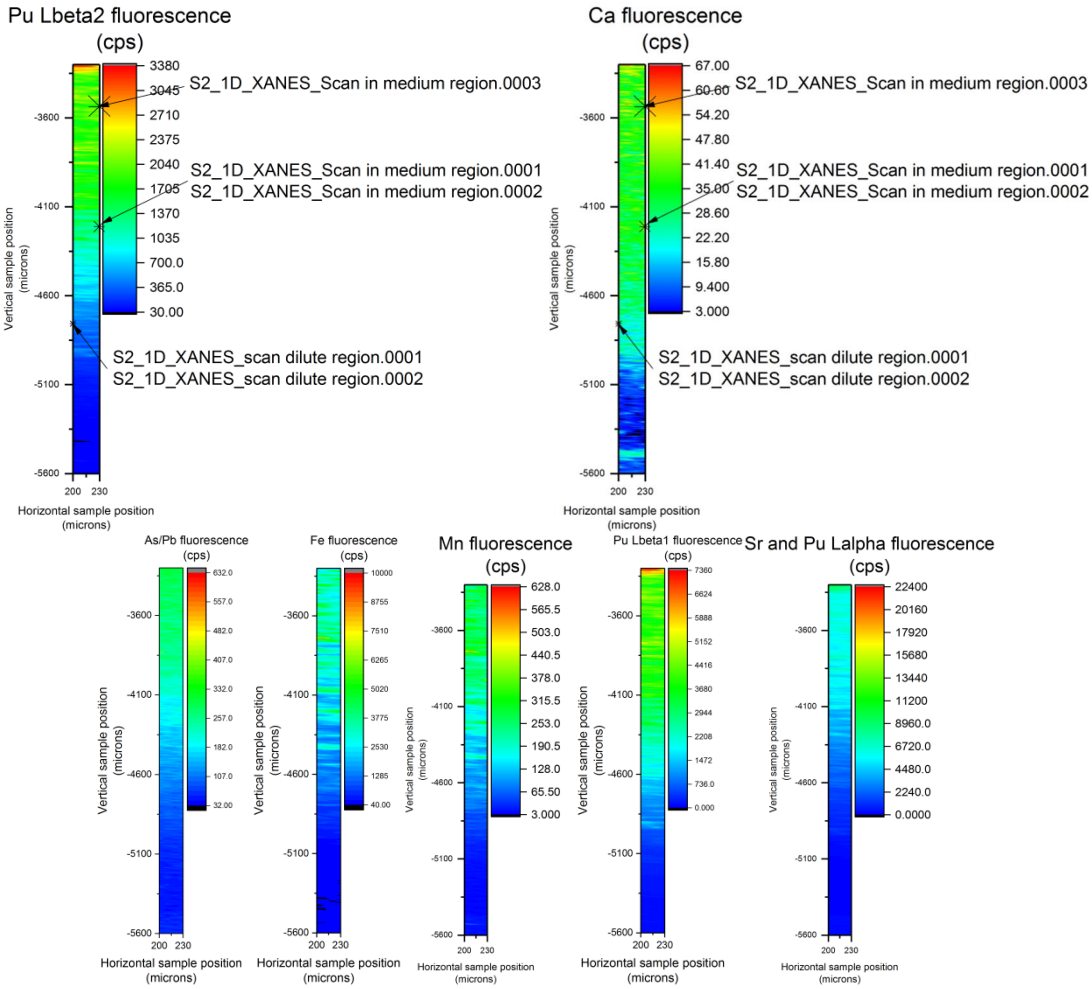

XRF map 1. Sample 2 leached, short cure sample. XRF map from unaltered core, across entire leached zone and onto calcite coated curved surface of sample.

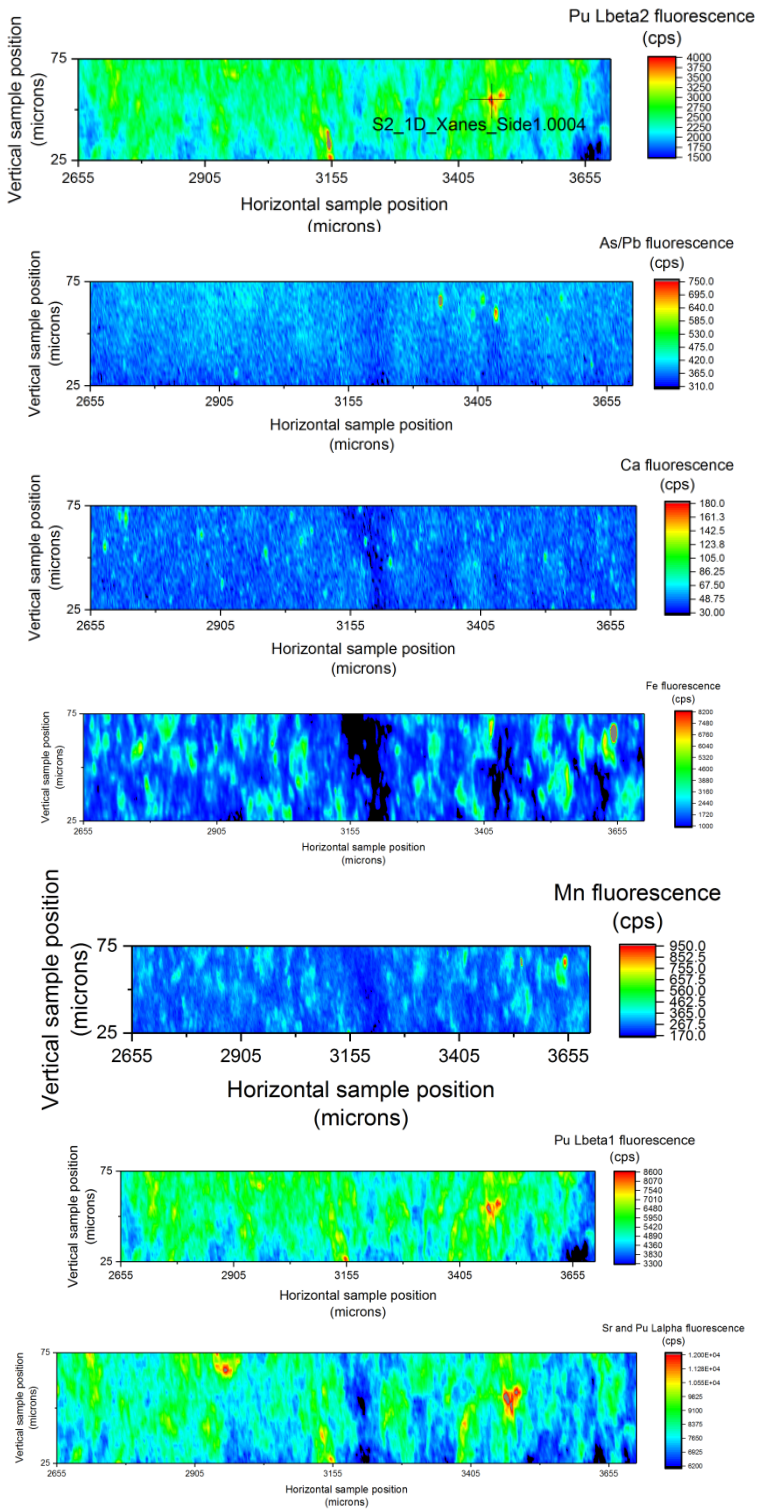

XRF map 2. Pu hotspot on top of Fe-rich cement grain with some Mn. XAS sampling spot adjacent (~150 microns) to leached layer boundary and is between the leached layer and a crack in the cement

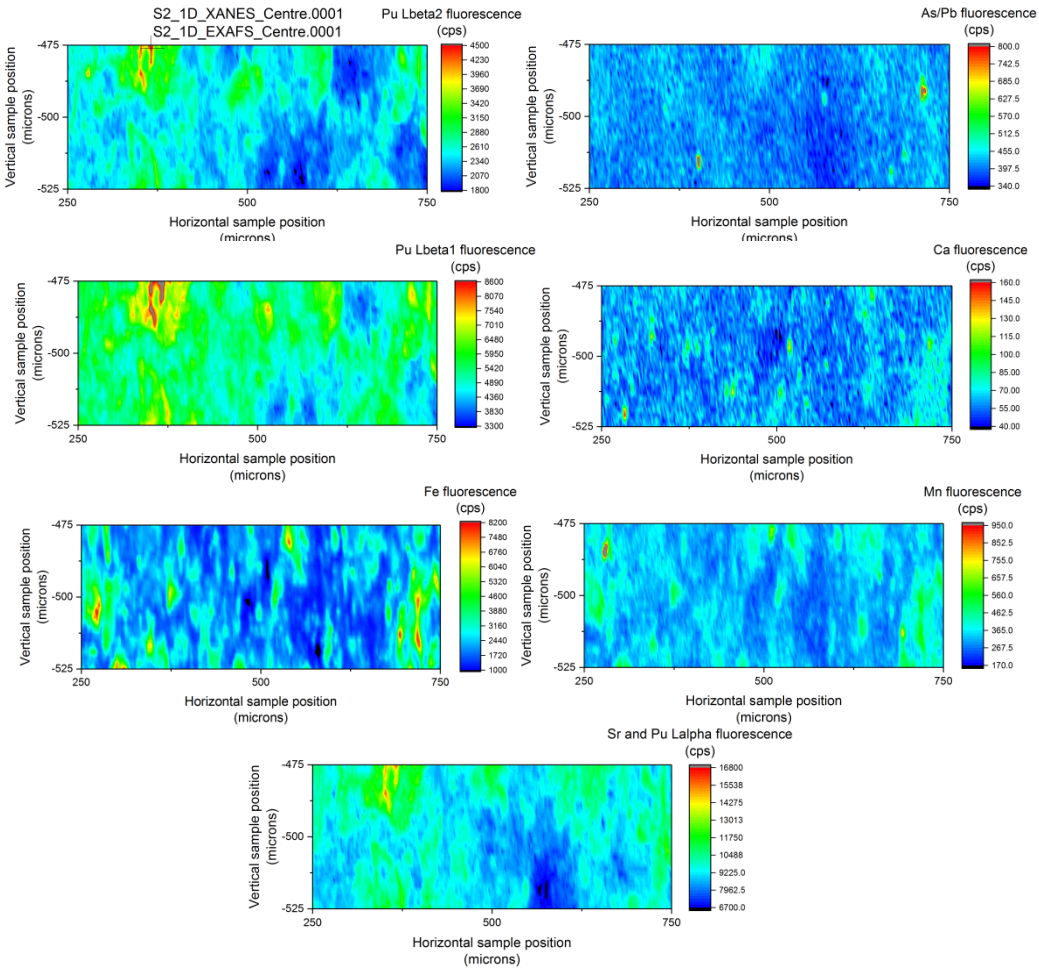

XRF map 3. XAS on high Pu concentration hotspot from center of unaltered core material, mix of Pu, Ca and cement forming elements. No obvious control over Pu distribution.

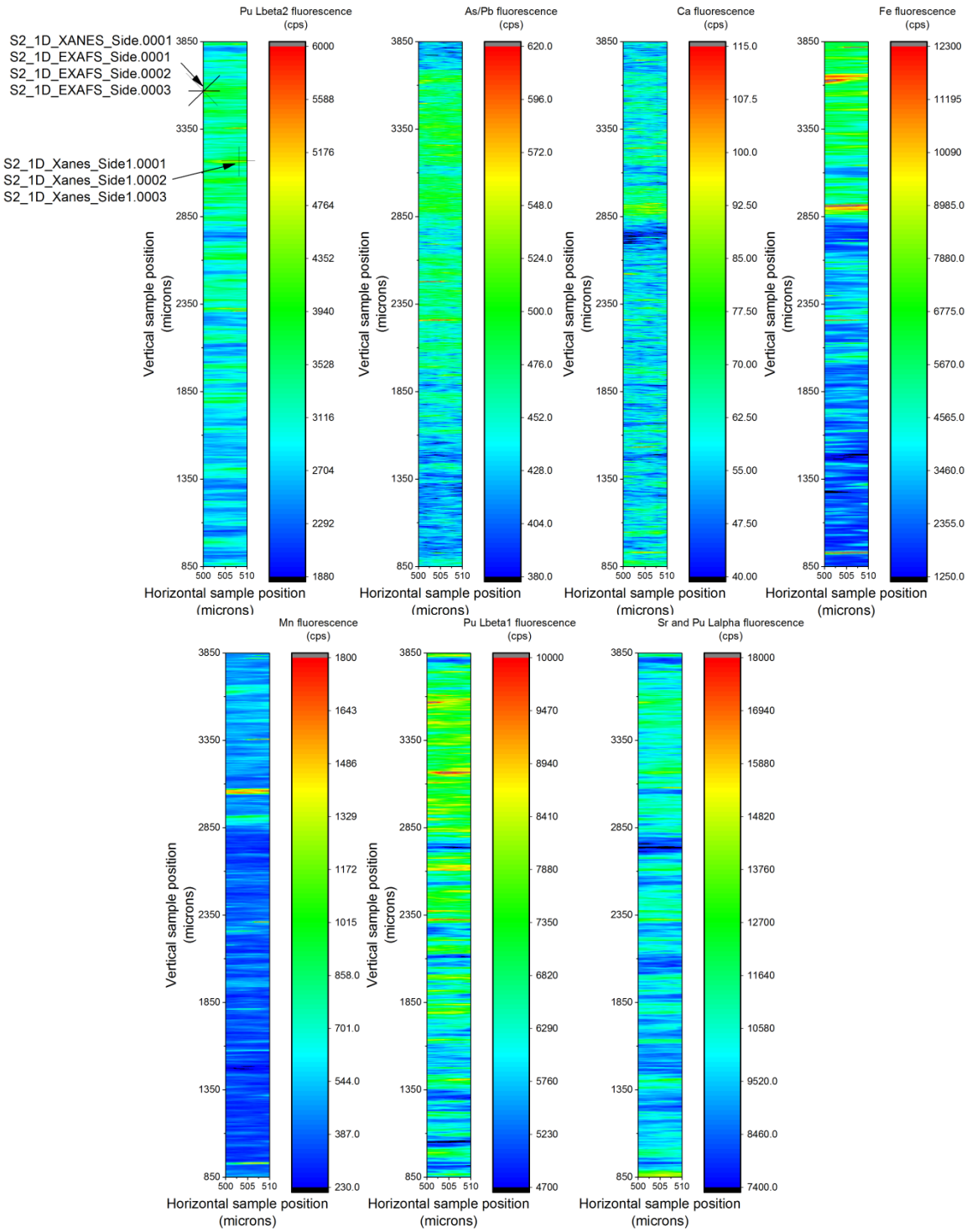

XRF map 4. Unaltered material with medium Pu concentration zone. Large Pu zone.

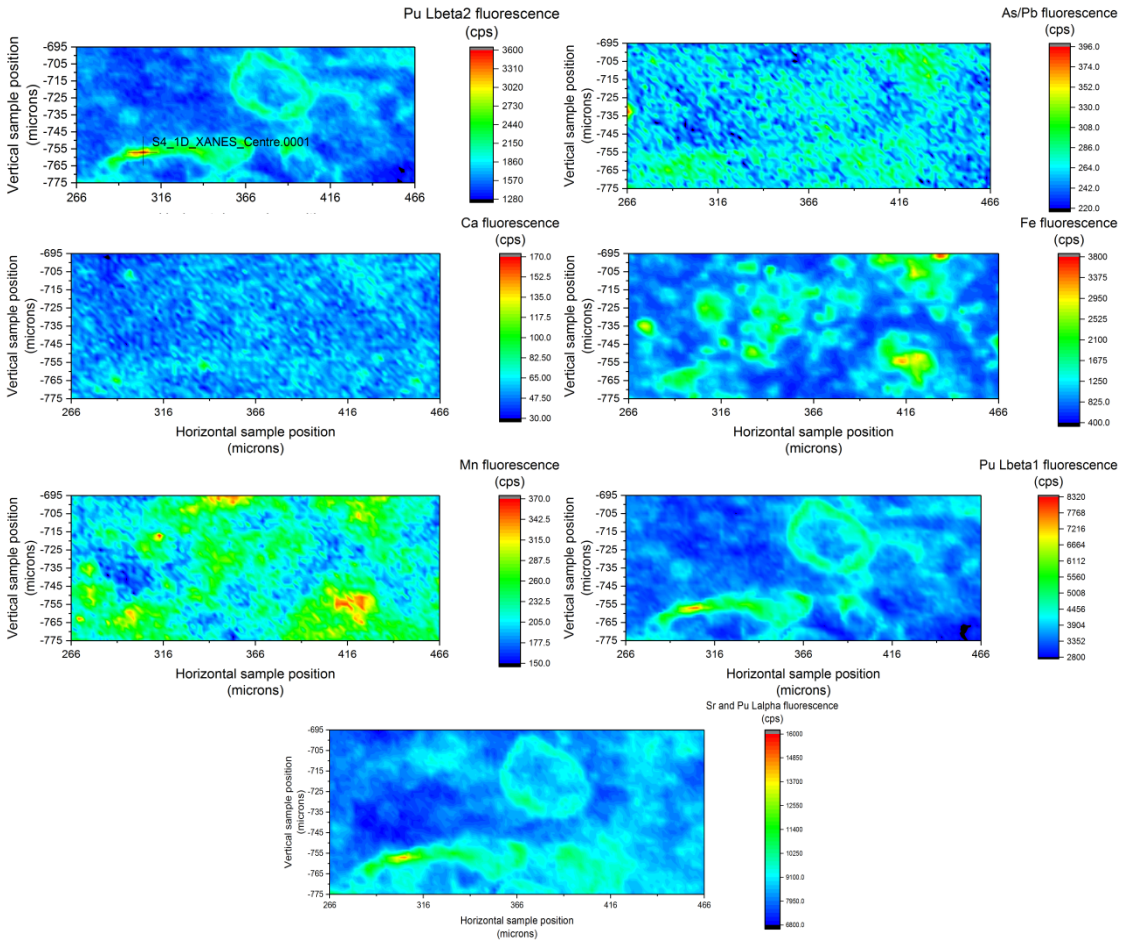

XRF map 5. XAS from high conc. Pu hotspot from Pu layer coating a Fe-rich cement grain.

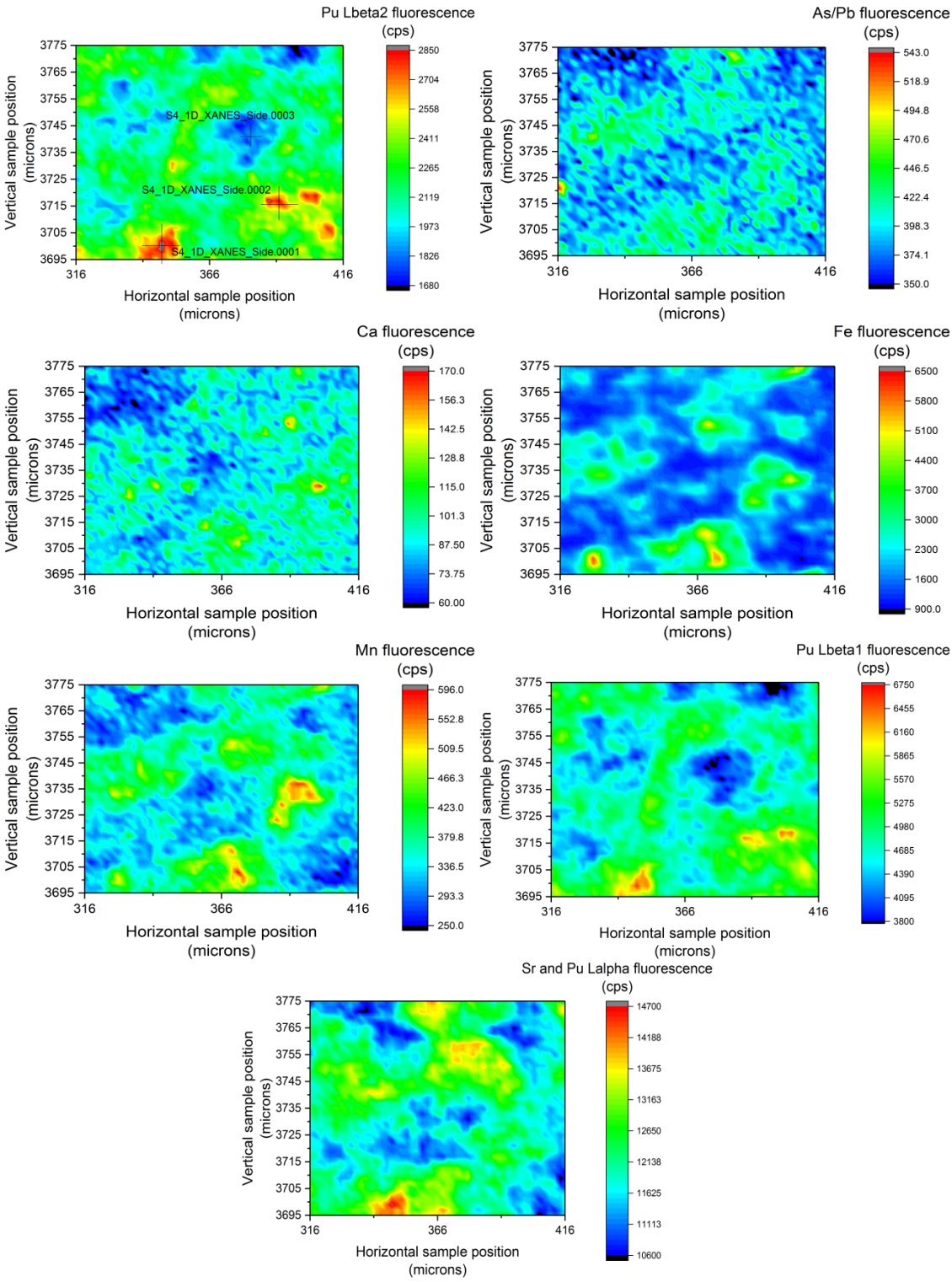

XRF map 6. XAS from high concentration Pu spot in large high concentration Pu area on Fe/Mn rich cement.

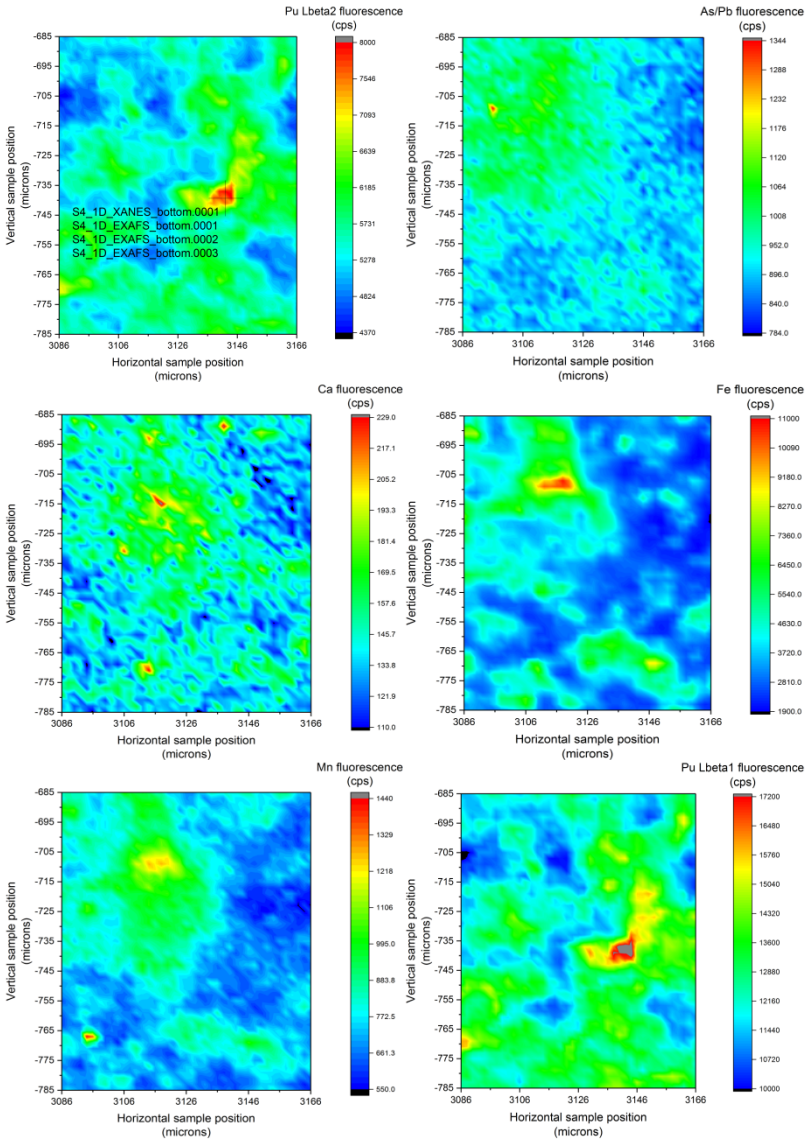

XRF map 7. XAS from high conc. Pu spot near to Ca-rich vein.

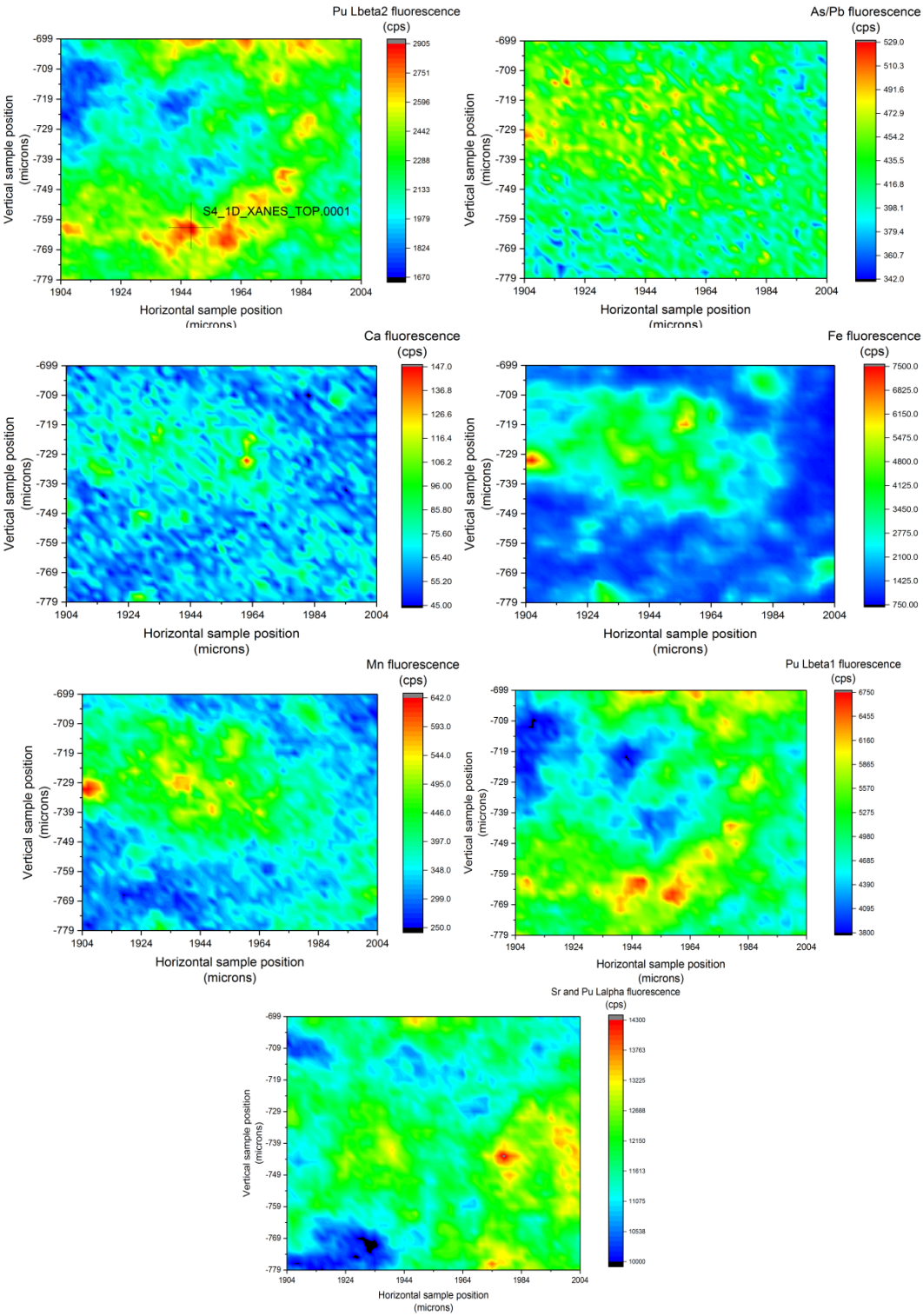

XRF map 8. Medium Pu concentration. XAS spot is in large area with high Pu concentration; lack of any fluorescence in other channels especially Fe and Mn fluorescence suggests that the Pu is incorporated into $Ca(OH)_2$ phase; from which the Ca fluorescence co-emission is blocked by the Pu.

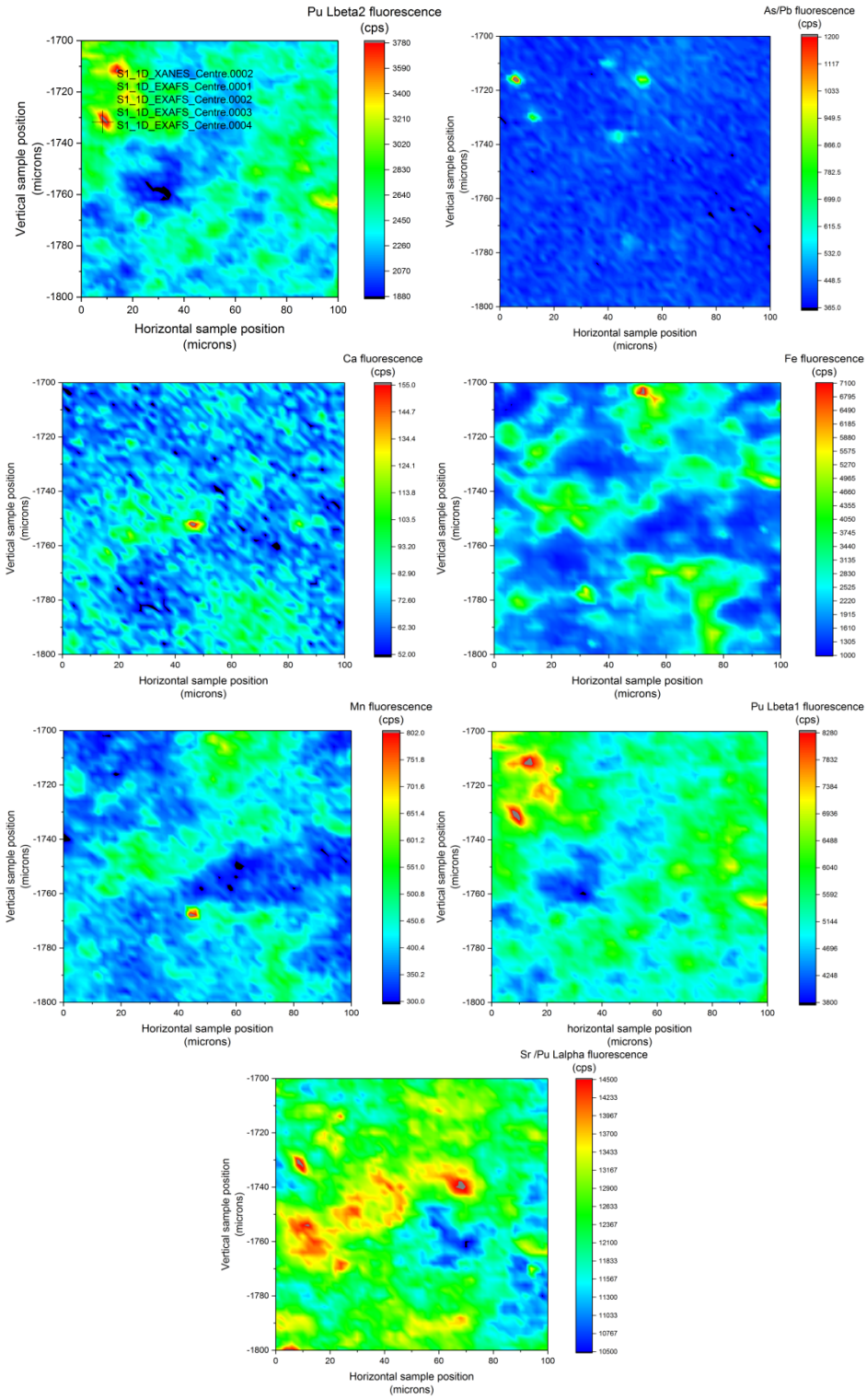

XRF map 9. Pu hotspot near to Fe/Mn-rich cement grain. The XRF shows very high Sr-rich regions not associated with the Pu-rich regions.

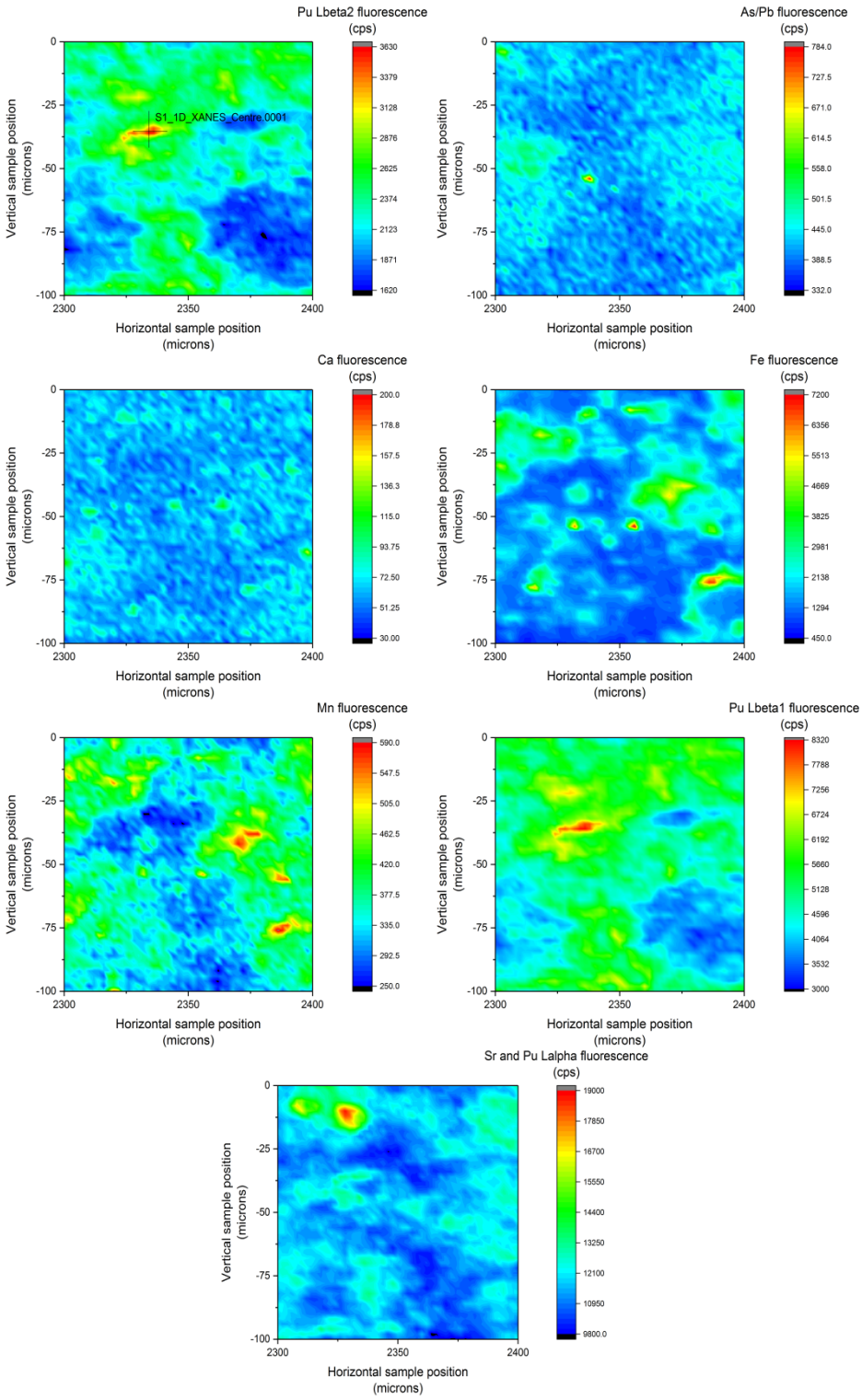

XRF map 10. High concentration Pu hotspot in middle of large mass of Pu material.

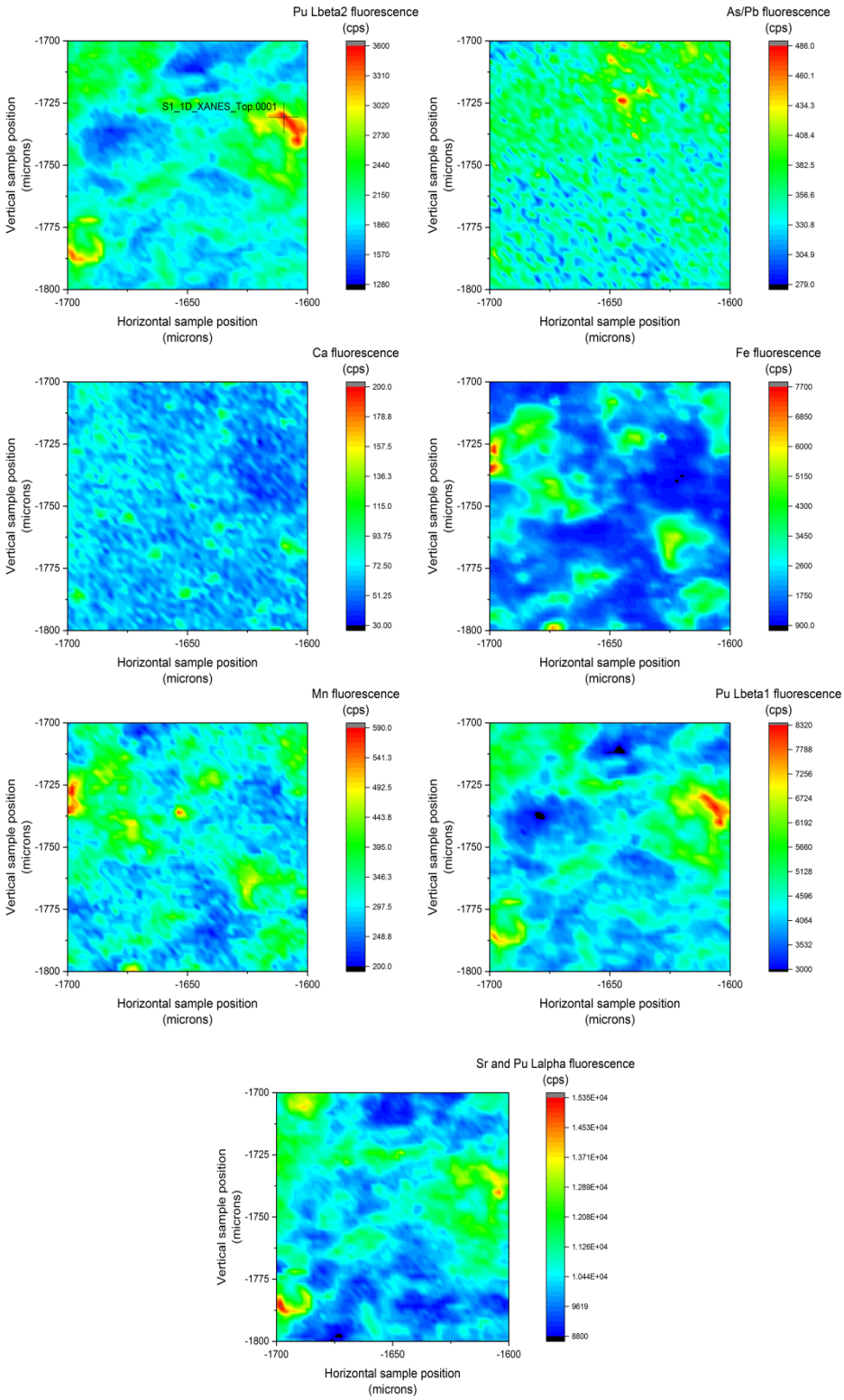

XRF map 11. High concentration Pu hotspot in middle of large mass of Pu-rich material.

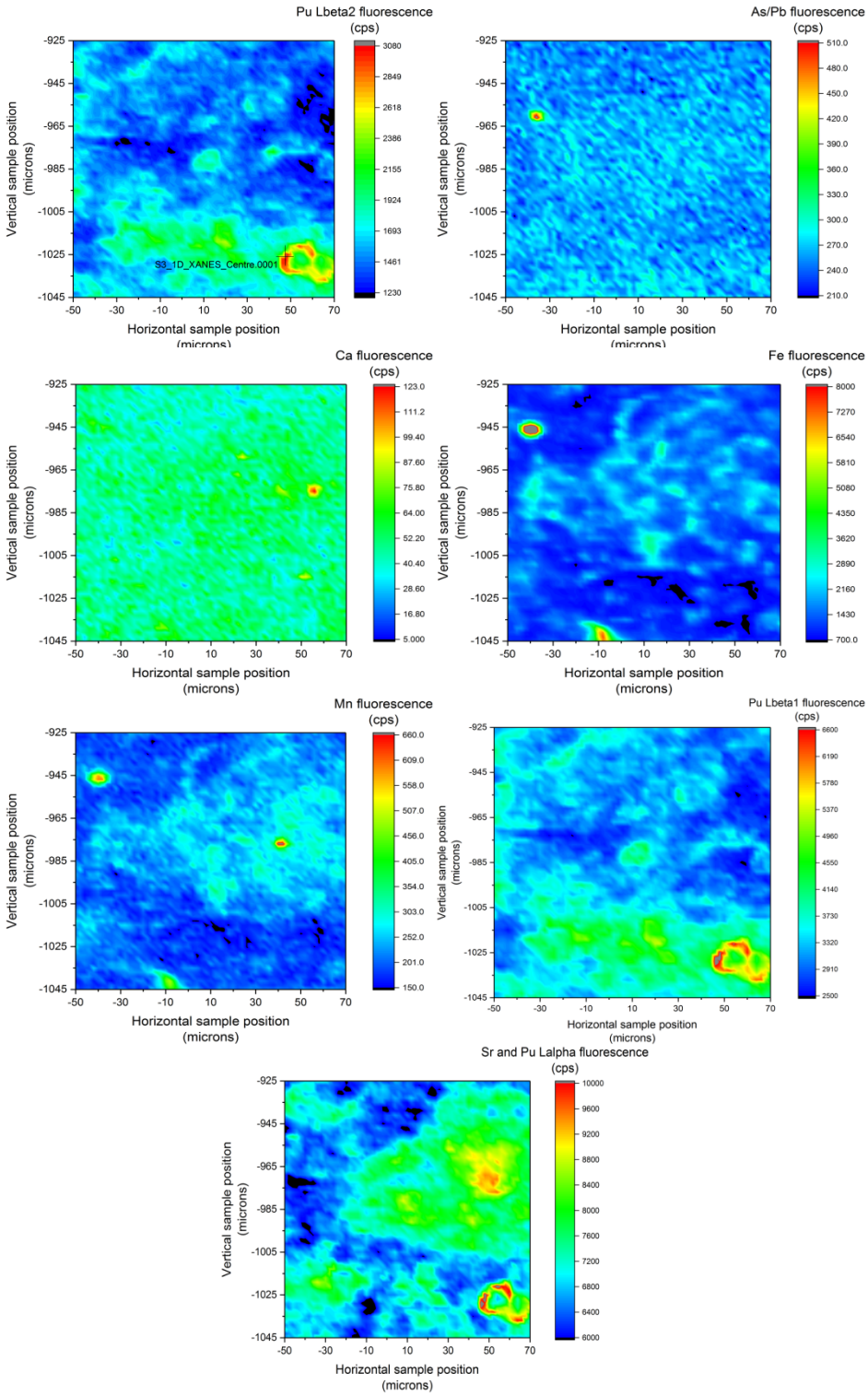

XRF map 12. XAS from high concentration Pu hotspot near to Sr/Fe rich cement grain.

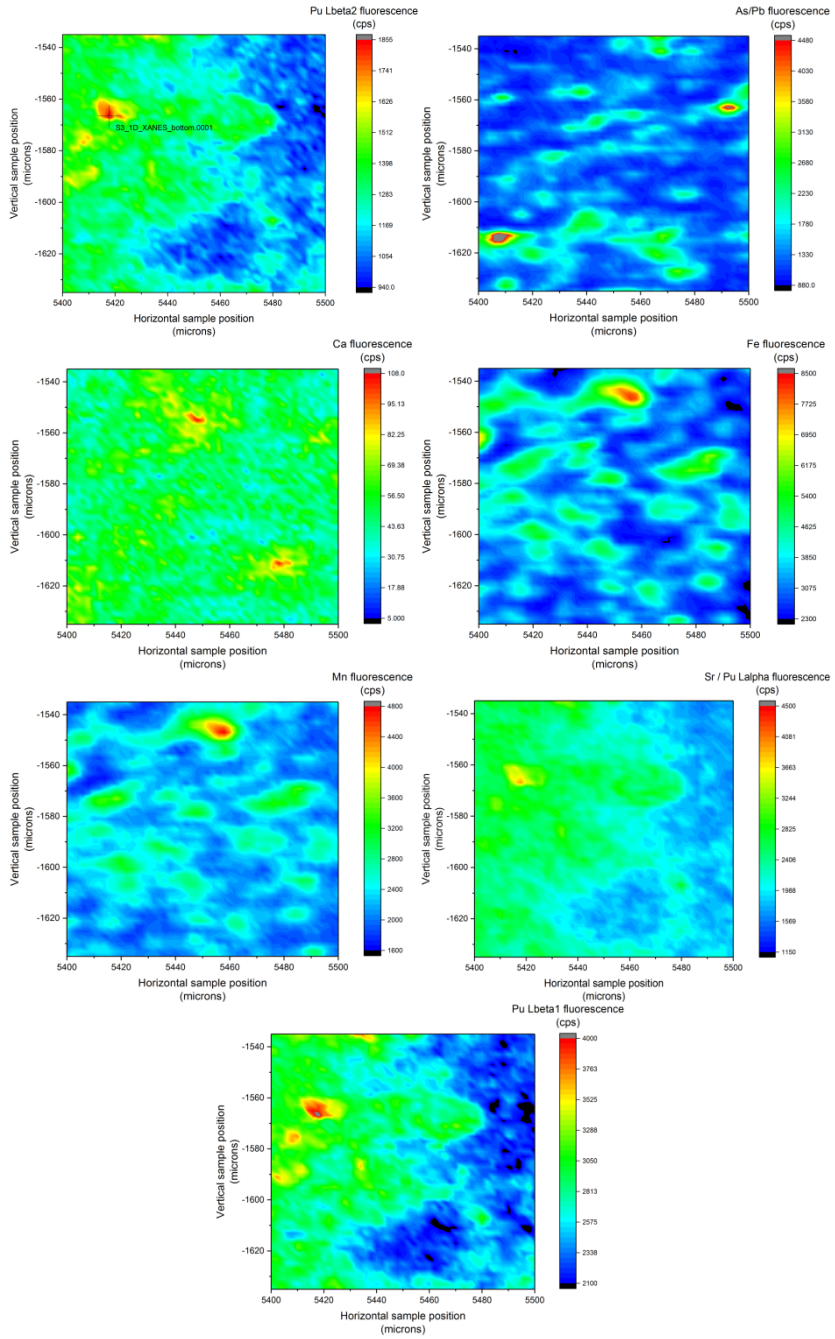

XRF map 13. XAS from the leached layer, location on the very edge of sample. High concentration Pu hotspot in large area of Pu material. Lots of Fe cement grains distributed. No obvious correlation between Pu and Fe distribution. Pu concentration gradient but not Fe or Ca.

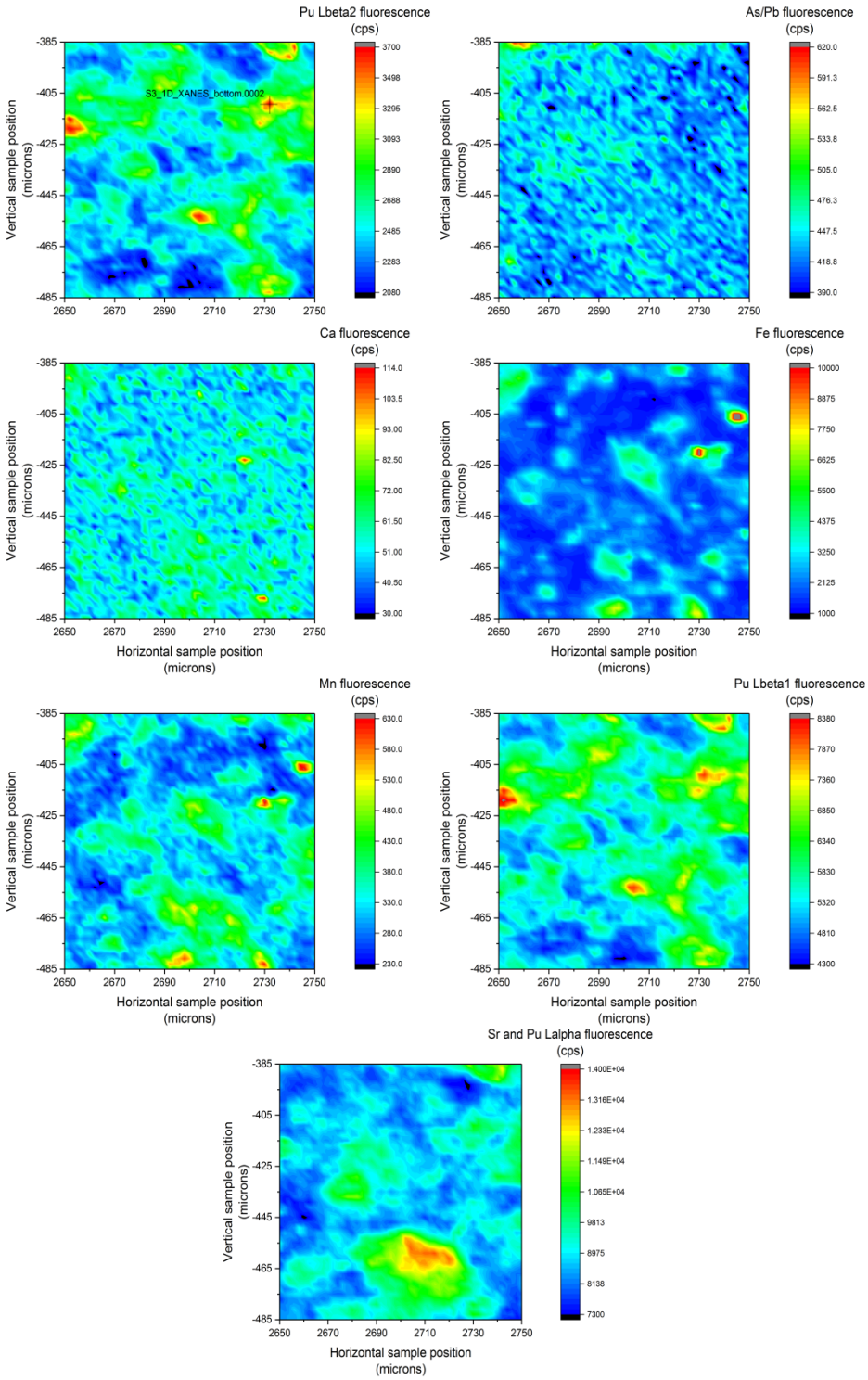

XRF map 14. Pu XAS in middle of leached area.

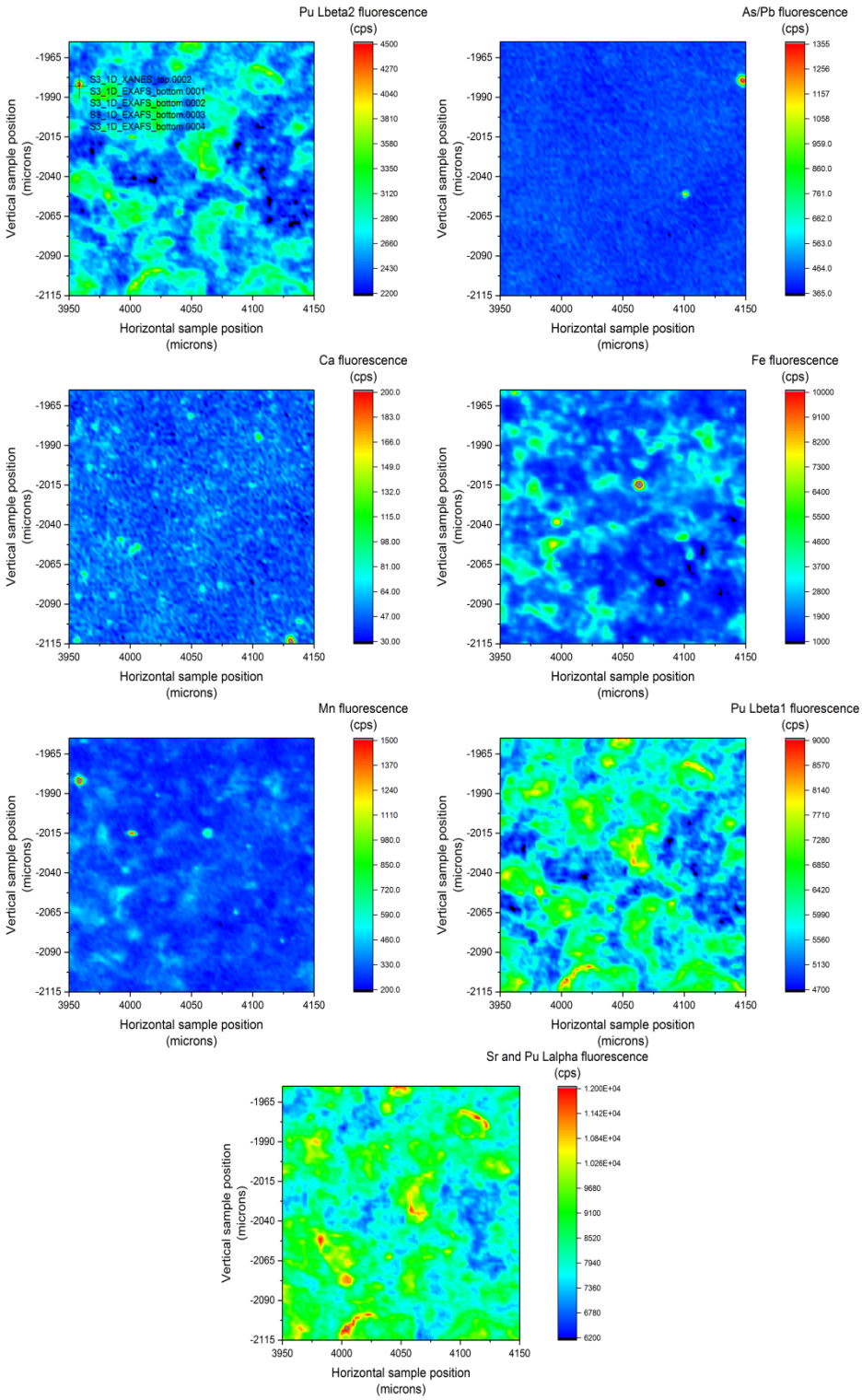

XRF map 15. Pu XAS in middle of leached area. High conc. Pu hotspot adjacent to Mn-rich grain

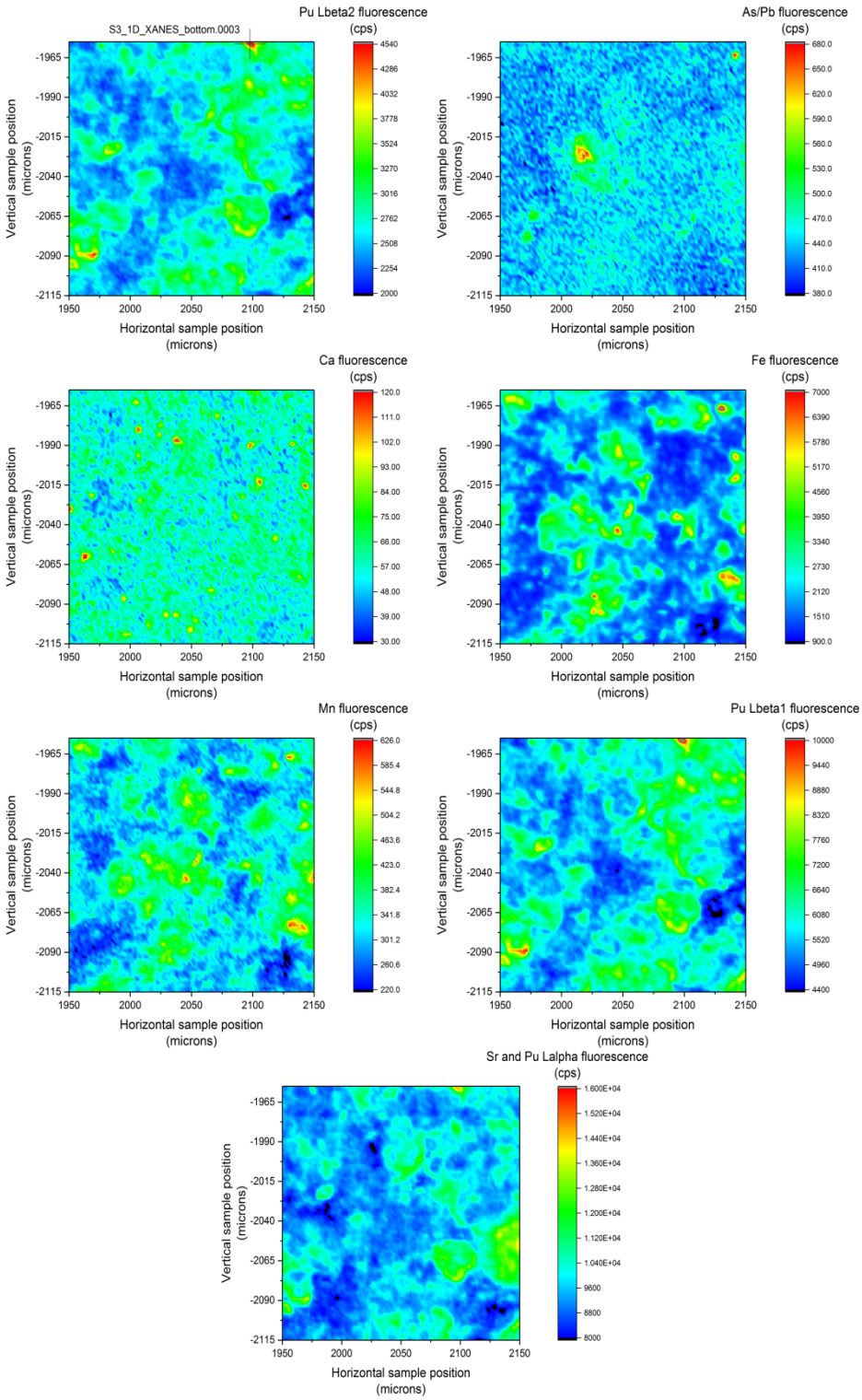

XRF map 16. XRF of unaltered material at edge of leached layer. XANES collected at Pu hotspot at the top of the map.

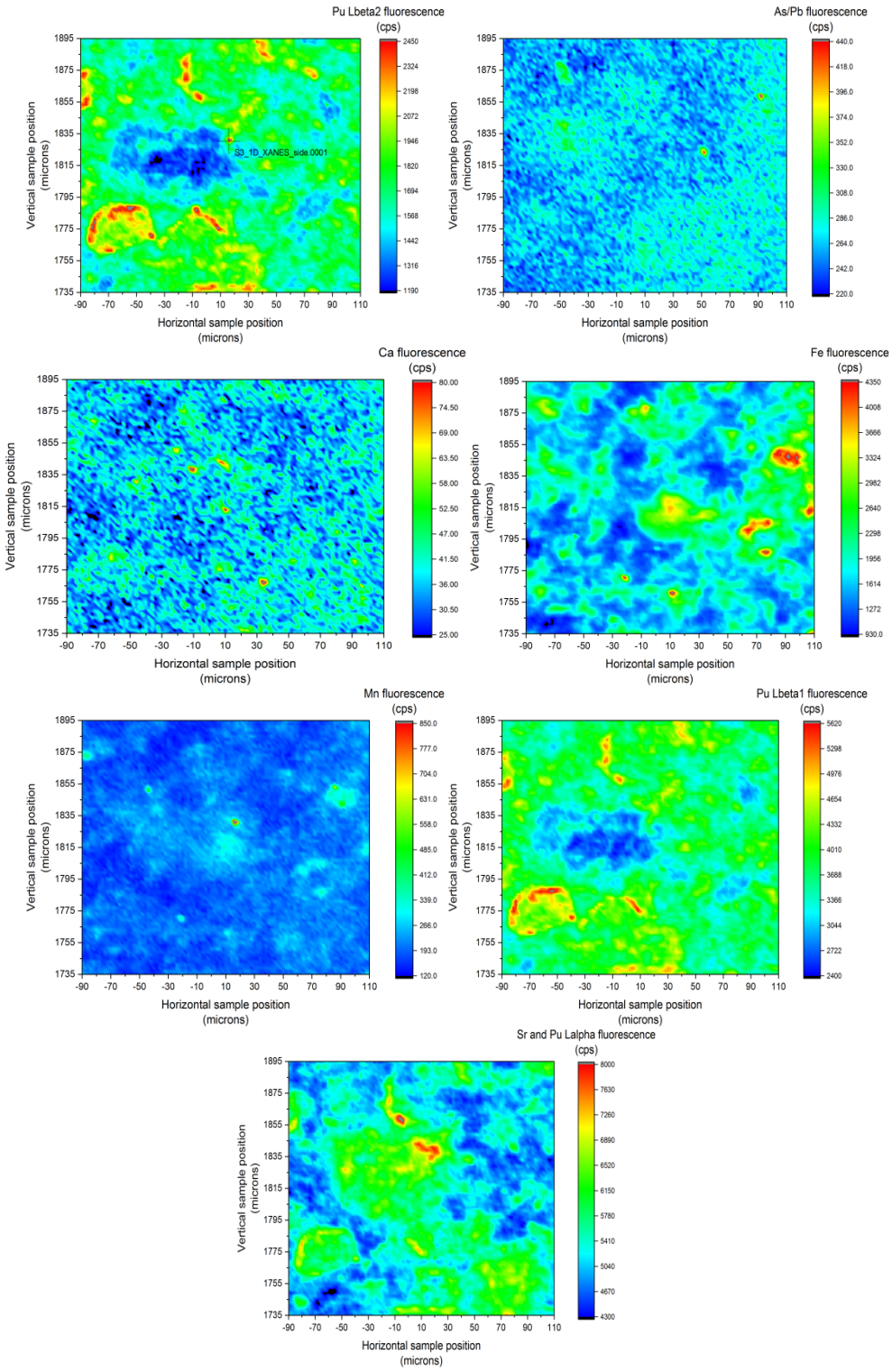

XRF map 17. Pu on top of Sr/Fe-rich cement grain; not the most concentrated Pu spot in the XRF map, so represents a medium Pu concentration zone.

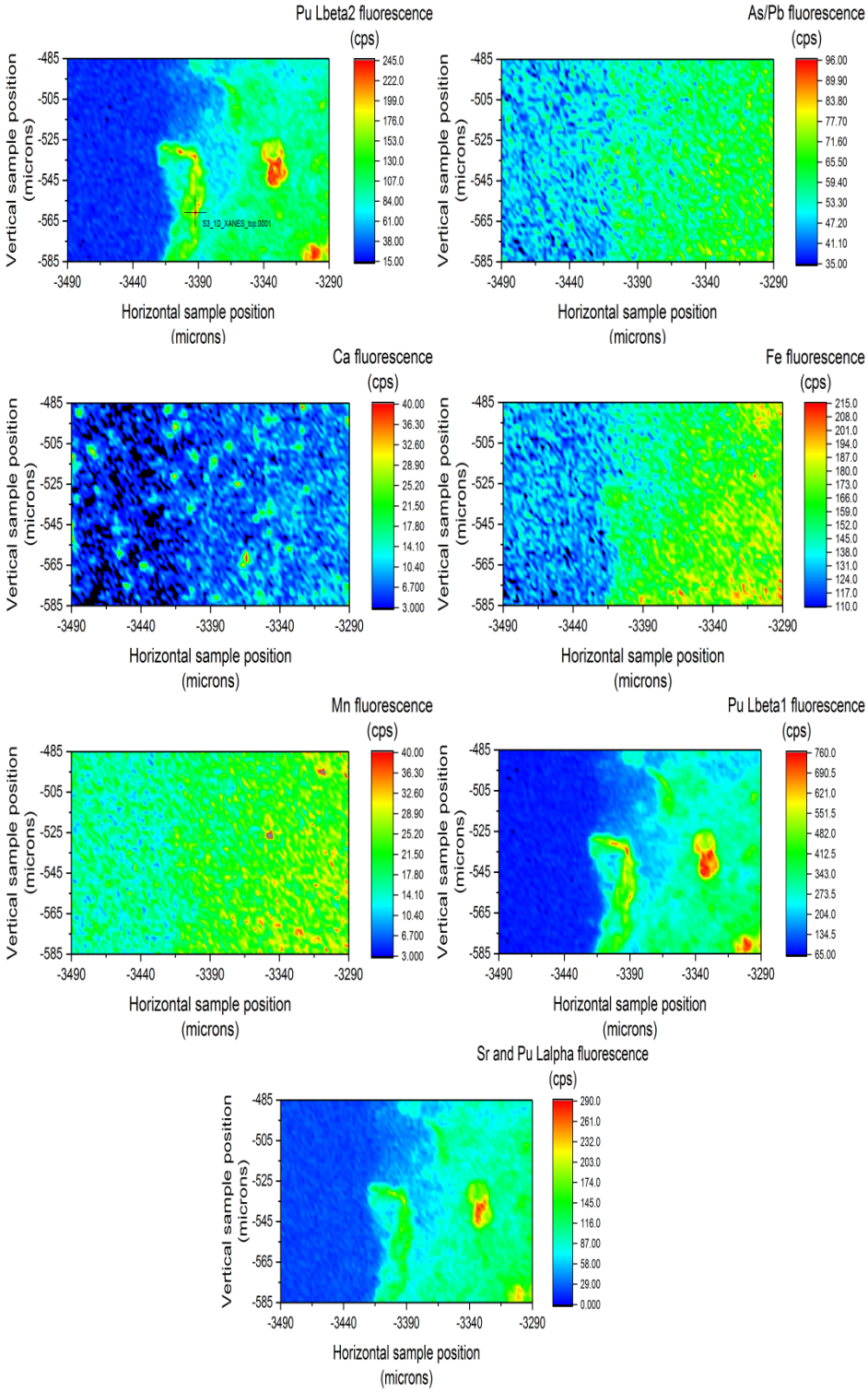

XRF map 18. Dilute concentration Pu at edge of core on boundary with leached layer. This shows the front of the advancing dissolution zone where the Pu and cement forming element are depleted.